ADVANCED MATERIALS

Supporting Information

for *Adv. Mater.,* DOI: 10.1002/adma.202105976

Biodegradable Polymer with Effective Near-Infrared-II Absorption as a Photothermal Agent for Deep Tumor Therapy

Yingjie Yu, Dongsheng Tang, Chaoyong Liu, Qi Zhang, Lin Tang, Yunfeng Lu,* and Haihua Xiao**

Supporting Information

Biodegradable Polymer with Effective Near-Infrared-II Absorption as a Photothermal Agent for Deep Tumor Therapy

Yingjie Yu, Dongsheng Tang, Chaoyong Liu, Qi Zhang, Lin Tang, Yunfeng Lu*, Haihua Xiao**

Dr. Y. Yu, L. Tang, Prof. C. Liu
State Key Laboratory of Organic-Inorganic Composites; Beijing Laboratory of Biomedical Materials; Beijing Advanced Innovation Center for Soft Matter Science and Engineering; College of Life Science and Technology, Beijing University of Chemical Technology, Beijing 100029, P.R. China
Email: chaoyongliu@mail.buct.edu.cn

D. Tang, Prof. H. Xiao
Beijing National Laboratory for Molecular Science, State Key Laboratory of Polymer Physical and Chemistry, Institute of Chemistry, Chinese Academy of Science, Beijing 100190, China
University of Chinese Academy of Science, Beijing 100049, China
Email: hhxiao@iccas.ac.cn

Dr. Q. Zhang

Department of Chemistry, University of Michigan, Ann Arbor, MI 48109, United States

Prof. Y. Lu
Department of Chemical and Biomolecular Engineering
University of California, Los Angeles,
Los Angeles, CA 90095, USA
E-mail: luucla@ucla.edu

SUPPLEMENTAL MATERIALS AND METHODS

1. Materials and Agents

All chemicals were obtained from commercial sources and used without further purification unless otherwise noted. 2,5-Bis(2-ethylhexyl)-3,6-bis(5-(trimethylstannyl)thiophen-2-yl)-2,5-dihydropyrrolo[3,4-c]pyrrole-1,4-dione, and 2,6-dibromo-4,4-bis(2-ethylhexyl)cyclopenta[2,1-b:3,4-b']dithiophene were purchased from Alfa Chemical *Co., Ltd.*(Zhengzhou, China), 4,9-Dibromo-6,7(4-hexylphenyl) [1,2,5]thiadiazolo[3,4-g]quinoxaline was purchased from Shanghai Tensus Biotech *Co., Ltd.*(Shanghai, China), Other reagents were purchased from Energy Chemical *Co., Ltd.*(Shanghai, China). $mPEG_{5000}$-$PLGA_{7600}$, Cy5.5, and Cy7.5 were purchased from Xi'an ruixi Biological Technology *Co.,Ltd*. (Xi'an, China).

Cell culture vessels were purchased from Corning (Corning, NY, USA). Modified Eagle's Medium (DMEM), RPMI-1640 medium, fetal bovine serum (FBS), 0.25% trypsin-EDTA, and penicillin/streptomycin (P/S) were purchased from (Gran Island, NY, USA). 3-(4,5-dimethylthiazol-2-yl)-2,5-diphenyltetrazolium bromide (MTT) were purchased from Aladdin (Shanghai, China). 2-(4-amidinophenyl)-1H-indole-6-carboxamidine (DAPI), propidium iodide (PI), Alexa fluor 488, TUNEL Apoptosis Assay Kit was purchased from Solarbio Science & Technology *Co.,Ltd.* (Beijing, China).

2. Characterization

^{1}H NMR spectra and ^{13}C NMR were measured by a 400 MHz NMR spectrometer (Bruker, Germany) at room temperature. FT-IR was characterized by Fourier Transform Infrared Spectrometer (Bruker, Germany). Molecular weight of polymer was characterized by gel permeation chromatography (GPC) (Waters, USA). The size distribution of NP was measured by dynamic light scatting analysis (DLS, Malvern Nano ZS90, UK). The morphology and element composition of NP were characterized by transmission electron microscope (TEM) (Hitachi HT 7700, Japan). The absorbance spectra and fluorescence spectra were measured using a ultraviolet-visible spectrometer (UV-vis, UV-2600, Shimadzu, Japan). Localization

of NP were performed using a confocal laser scanning microscope (LSM-800, ZEISS, Germany). Cellular uptake of NP was measured with a CytoFLEX Flow Cytometer (Beckman Coulter, USA). The MTT assay was conducted using a Microplate reader (SpectraMax, USA). *In vivo* imaging was conducted by an *In Vivo* Imaging System (IVIS, Perkin Elmer, USA).

3. Synthesis

1). Disulfanediylbis(ethane-2,1-diyl)bis(5-bromothiophene-2-carboxylate)

The mixture of 5-bromothiophene-2-carboxylic acid (4.02 g, 19.42 mmol), bis(2-hydroxyethyl) disulfide (1.00 g, 6.48 mmol), EDC (3.73 g, 19.42 mmol) and DMAP (2.37 g, 19.42 mmol) in DMF (30 ml) was stirred for 4 h at room temperature under N_2 atmosphere. Then, the mixture was quenched with deionized water and further extracted with ethyl acetate. After extraction, the organic phase was evaporated, and the crude product was obtained as light-yellow oil. The oily product was purified with chromatography on silica gel (CH_2Cl_2/EA = 9:1) to afford white powder (2.41 g, 70.3% yield). ^{1}H NMR (300 MHz, $CDCl_3$): δ ppm 7.56 (d, 2H), 7.08 (d, 2H), 4.56 (t, 4H), 3.06 (t, 4H). ^{13}C NMR (75 MHz, CDCl3): δ ppm 160.78, 134.31, 134.06, 131.02, 120.75, 63.09, 37.19. ES MS (m/z): calcd for $[C_{14}H_{12}Br_2O_4S_4+Na]^+$: 554.7862; found, 554.7854.

2). Butane-1,4-diyl bis(5-bromothiophene-2-carboxylate)

In a 100 ml round bottom flask, the mixture of 5-bromothiophene-2-carboxylic acid (6.85 g, 33.30 mmol), 1,4-butanediol (1.00 g, 11.10 mmol), EDC (6.38 g, 33.30 mmol) and DMAP (4.06 g, 33.30 mmol) in DMF was stirred for 4 h at room temperature under N_2 atmosphere. Then, the mixture was quenched with deionized water and further extracted with ethyl acetate. After extraction, the organic phase was evaporated, and the crude product was obtained as light-yellow oil. In the following, the oily product was purified with chromatography on silica gel (CH_2Cl_2/EA = 9:1) to afford white powder (3.53 g, 68.3% yield). ^{1}H NMR (300 MHz, CDCl3): δ ppm 7.55 (d, 2H), 7.08 (d, 2H), 4.34 (t, 4H), 1.88 (t, 4H). ^{13}C NMR (75 MHz, CDCl3): 161.01, 134.81, 133.66, 130.94, 120.30, 64.76, 25.39. ES MS (m/z): calcd for $[C_{14}H_{12}Br_2O_4S_2+Na]^+$: 490.8421; found, 490.8415.

3). P0

Compound M1 (69.18 mg, 0.081 mmol), compound M2a (22.80 mg, 0.041 mmol), compound M2b (27.11 mg, 0.041 mmol), p(o-tol)$_3$ (1.97 mg, 0.0065 mmol), and dba$_3$Pd$_2$ (1.47 mg, 0.0016 mmol) were added into a 25 ml Schlenk tube equipped with a magnetic stirrer. Toluene (8 ml) was then added into the tube, and the solution was deoxidized with nitrogen for 25 min. The polymerization reaction was carried out at 120 ℃ under nitrogen atmosphere in dark for 30 min. The resulting solution was precipitated into 500 ml methanol and the solid was filtered and purified by Soxhlet extraction using methanol, acetone, hexane, and tetrahydrofuran sequentially, obtaining product P0 as a dark blue solid.

4). P10

Compound M1 (80.80 mg, 0.095 mmol), compound M2a (21.30 mg, 0.038 mmol), compound 2b (31.99 mg, 0.048 mmol), compound M3 (5.03 mg, 0.0095 mmol), p(o-tol)$_3$ (2.31 mg, 0.0076 mmol), and dba$_3$Pd$_2$ (1.73 mg, 0.0019 mmol) were added into a 25 ml Schlenk tube equipped with a magnetic stirrer. Toluene (6 ml) was then added into the tube, and the solution was deoxidized with nitrogen for 25 min. The polymerization reaction was carried out at 120 ℃ under nitrogen atmosphere in dark for 30 min. The resulting solution was precipitated into 500 ml methanol and the solid was filtered and purified by Soxhlet extraction using methanol, acetone, hexane, and tetrahydrofuran sequentially, obtaining the P10 as the dark blue solid.

5). P30

Compound M1 (119.50 mg, 0.14 mmol), compound M2a (15.69 mg, 0.028 mmol), compound M2b (46.66 mg, 0.07 mmol), compound M3 (22.25 mg, 0.042 mmol), p(o-tol)$_3$ (3.35 mg, 0.011 mmol), and dba$_3$Pd$_2$ (2.56 mg, 0.0028 mmol) were added into a 25 ml Schlenk tube equipped with a magnetic stirrer. Toluene (7 ml) was then added into the tube, and the solution was deoxidized with nitrogen for 25 min. The polymerization reaction was carried out at 120 ℃ under nitrogen atmosphere in dark for 1 h. The resulting solution was precipitated into 500 ml methanol and the solid was filtered and purified by Soxhlet extraction using methanol, acetone, hexane, and tetrahydrofuran sequentially to obtain the P30 as the dark blue solid.

6). P70

Compound M1 (48.55 mg, 0.057 mmol), compound M2a (4.82 mg, 0.0086 mmol), compound M2b (5.73 mg, 0.0086 mmol), compound M3 (21.19 mg, 0.040 mmol), $p(o\text{-}tol)_3$ (1.40 mg, 0.0046 mmol), and dba_3Pd_2 (1.01 mg, 0.0011 mmol) were added into a 25 ml Schlenk tube equipped with a magnetic stirrer. Toluene (5 ml) was then added into the tube, and the solution was deoxidized with nitrogen for 25 min. The polymerization reaction was carried out at 120 ℃ under nitrogen atmosphere in dark for 4 h. The resulting solution was precipitated into 500 ml methanol and the solid was filtered and purified by Soxhlet extraction using methanol, acetone, hexane, and tetrahydrofuran sequentially to obtain the P70 as the blue solid.

7) P30 analogue (non-degradable polymer)

Compound M1 (107.93 mg, 0.13 mmol), compound M2a (14.57 mg, 0.026 mmol), compound M2b (43.32 mg, 0.065 mmol), compound non-degradable (18.17 mg, 0.039 mmol), $p(o\text{-}tol)_3$ (3.04 mg, 0.010 mmol), and dba_3Pd_2 (2.38 mg, 0.0026 mmol) were added into a 25 ml Schlenk tube equipped with a magnetic stirrer. Toluene (8 ml) was then added into the tube, and the solution was deoxidized with nitrogen for 25 min. The polymerization reaction was carried out at 120 ℃ under nitrogen atmosphere in dark for 1 h. The resulting solution was precipitated into 500 ml methanol and the solid was filtered and purified by Soxhlet extraction using methanol, acetone, hexane, and tetrahydrofuran sequentially, obtaining the non-degradable polymer as a dark blue solid.

8). NP

To prepared NP, P30 (0.3 mg) and PEG-PLGA (3 mg) were dissolved in THF (1 ml) and mixed uniformity to work as the stock solution. Then the stock solution was added dropwise into a mixture of deionized water (9 ml) and THF (1 ml) during continuous sonication. THF was then removed by evaporation under nitrogen flow for 30 mins. Subsequently, the aqueous solution was filtered through a 0.22 μm polyvinylidene fluoride (PVDF) syringe. The prepared NP were stored in 4 °C freezer for the following usage. To prepare the fluorescent NP for confocal and *in vivo* imaging, Cy5.5 or Cy7.5 (4 μg) was co-dissolved with P30 (0.3 mg) in THF. The following preparation process is same as the beforementioned NP

preparation procedure.

4. Photothermal measurement

The photothermal performance of polymers and NP were carefully evaluated. The polymers (P0, P10, P30, and P70) were dissolved in THF solution at concentration of 200 μg ml^{-1}. NP aqueous solutions with various concentration (6.25, 12.5, 25, 50, 100, and 200 μg ml^{-1}) were prepared. Then the NP aqueous solution was irradiated by 808 nm laser or 1064 nm laser for 8 min, respectively. The temperature profiles and images were precisely recorded with a FOTRIC 225S infrared thermal camera.

To obtain the photothermal conversion efficiency (η) for polymer solution or NP dispersion, the heating curve of various polymer solutions was monitored. Polymer solution or NP dispersion was recorded upon 808 nm or 1064 nm laser irradiation (1 W cm^{-2}) for 8 min to achieve the maximum plateau of temperature, and the laser was turned off for natural cooling to room temperature. Thus, η can be calculated referring to the following Equation (1):

$$\eta = \frac{hS(T_{max}-T_{surr})-Qdiss}{I(1-10^{A_\lambda})} \quad \cdots\cdots \quad (1)$$

Where h is the heat transfer coefficient; S is the surface area of the used holder; T_{max} and T_{surr} denote the maximum steady-state temperature and room temperature of the ambient environment, respectively; Q_{Diss} is the heat wastage form the light loss of the solvent and holder; I is the laser intensity (1 W cm^{-2}), and A_λ represents the absorbance of corresponding NP aqueous dispersion at 1064 nm. hS can be calculated referring to the following Equation (2):

$$\tau_s = \frac{mC_p}{hS}, \quad \cdots\cdots \quad (2)$$

Where τ_s is the time constant, m is the mass of the solution, and C_p is the heat capacity of corresponding solvent. Finally, the PCE can be calculated from the method above.

5. Cyclic voltammetry (CV) measurements

Three-electrode cell with Ag/AgCl as the reference electrode was applied on a CHI660C

electrochemical workstation. The scan rate was 100 mV/s, nitrogen bubbled solution of *tetra-n*-butylammonium hexafluorophosphate (0.1 M in acetonitrile) was used as electrolyte solution. For calibration, the redox potential of ferrocene/ferrocenuim (Fc/Fc^+) was measured under the same conditions. The respective onset oxidation (E_{ox}^{onset}) and reduction potentials (E_{red}^{onset}) were measured. HOMO and LUMO energies of these conjugated polymers were estimated with the following equations: HOMO = -(E_{ox}^{onset} + 4.80) eV, LUMO = -(E_{red}^{onset} + 4.80) eV. The bandgaps were estimated with their HOMO/LUMO levels ($E_g^{cv} = E_{LUMO} - E_{HOMO}$). All the data are listed in Table S2.

6. Cell culture

The RPMI-1640 and Modified Eagle's Medium (DMEM) medium was mixed with 10% fetal bovine serum (FBS) and 1% antibiotics (penicillin and streptomycin) for the culture of OVCAR8 cells. The culture condition is 37 °C in a humidified environment containing 5% CO_2. For cell harvesting, 0.5% w/v trypsin in phosphate-buffered saline (PBS) was used to detach from the cell culture dish, and then resuspended in fresh medium for the following usage.

For multicellular spheroids cell culture, 1×10^3 mixed cells were seeded into agarose pre-coated 96-well plate and incubated at 37 °C in humidified atmosphere with 5% CO_2 for forming multicellular spheroids. After 8 days of growth, the cell spheres were basically formed.

***7. In vitro* Cytotoxicity**

The OVCAR8 cell line was seeded into the 96-well plates at a density of 5000 cells per well. After incubation for 24 h, NP solution with different concentrations (6.25, 12.5, 25, 50, 100, and 200 μg/ml) were added to the culture medium, respectively. 6 h later, cells were irradiated with or without laser (808 nm and 1064 nm) for 8 min. The treated cells were incubated for 24 h, then the standard MTT assay was employed to evaluate the performance of PTT. Briefly, MTT reagent (10 μL of 5 mg/ml solution in PBS buffer) was added to each well and the plates were incubated for another 4 h. Measurements of absorbance were subsequently completed with a Bio-Rad plate reader (SpetraMax M3) at 570 nm (peak

absorbance) and at 650 nm (background absorbance).

8. Intracellular Uptake of Cy5.5 labeled NP

For CLSM, OVCAR8 cells (5×10^5) were seeded in 6-well plates and cultured for 12 h. After incubation with Cy5.5 labeled NP at 37 °C for 1, 4, and 7 h, the cells were fixed with 4% (W/V) paraformaldehyde for 30 min. The cell nucleus was then stained with DAPI (2 μg/ml) for 5 min. In the end, images were collected with confocal laser scanning microscopy.

Flow cytometry was employed for quantification of the uptake process. OVCAR8 cells were cultured in 12-well plates (3×10^5 cells/well). Cy5.5 labeled NP was incubated with cells for 1, 4, and 7 h. The cells were then washed twice with cold PBS, lysed with trypsin–EDTA solution, collected by centrifugation (1500 rpm for 5 min), and analyzed for fluorescence intensity *via* flow cytometer.

9. Live/Dead Cell Staining

OVCAR8 cells were treated with the NP incubation and laser irradiation. The treated cells were then stained with a PBS buffer containing Calcein-AM and PI for 30 min in the cell-cultured container. After PBS wash, the cell samples were imaged on CLSM with the excitation at 488 nm and 532 nm, respectively.

The cell spheroids of OVCAR8 cells were obtained, with six cell spheroids in each group. Then cells were divided into 6 groups for the cytotoxicity study: 1) PBS, 2) 808 nm, 3) 1064 nm, 4) NP, 5) NP+808 nm, 6) NP+1064 nm. Groups 2, 5, and 6 were treated with NP at concentration of 50 μg/mL. Group 2 and 5 were irradiated with 808 nm laser (1 W cm^{-2}). Group 3 and 6 were irradiated with 1064 nm (1 W cm^{-2}). Before imaging by a CLSM, the cell spheroids were washed thoroughly with PBS and then stained with Calcein/PI Cell Viability/Cytotoxicity Assay Kit.

10. Deep-tissue photothermal study

To compare the penetration capacity of NIR-I and NIR-II laser, we used chicken breast

with different thickness to simulate the clinical condition. 400 µl of NP solution (100 µg ml^{-1}) was filled in a 24 well plate, covered by chicken breast tissue of various thicknesses (3, 6, and 9 mm) on top, and then exposed to 808 or 1064 nm laser for 8 min. Temperature of NP solution under chicken breast tissue was monitored by an IR thermal camera.

11. Establishment of Orthotopic HGSOC Model

The 6 weeks female BALB/c nude mice were used for imaging and efficacy studies upon establishment of a cell-line orthotopic xenograft model of high-grade serous ovarian cancer cells (HGSOC, 3×10^6 LUC^+ OVCAR8 cells/animal, 0.2 ml, intraperitoneal injection).

12. Procedure for image guided PTT on orthotopic HGSOC model

After the LUC signals from their tumors reached 3×10^6 radians (photons/sec/cm^2/surface area), the mice bearing LUC^+ OVCAR8 tumors were administrated with Cy7.5 labeled NP (200 µl, 500 µg/ml), or saline (200 µl) *via* IP injection. After 24 h, LUC and fluorescence imaging (Cy7.5) proceeded using an IVIS. The location of tumors was visualized *via in vivo* image of LUC signals upon injection of d-luciferin (50 mg/kg). The *in vivo* biodistribution of NP was observed on the Cy7.5 channel (λ_{ex}= 740 nm; λ_{em} = 840 nm). Thereafter, based on the BLI image, PTT was carried out by irradiating 808 nm or 1064 nm laser directly on the tumor region. IR thermal camera was employed to monitor the temperature of tumor region during laser irradiation. Upon completion of *in vivo* imaging, the mice were sacrificed and their organs were harvested and imaged *ex vivo* using the same parameters. The average photon flux in radians for the different reporter signals in each excised organ were quantified. The relative signal intensity distribution in each organ (after normalization to the signal intensity recorded from the tumor) was determined.

13. Antitumor Efficacy on the Orthotopic HGSOC Model

Once the LUC signals from their tumors reached 3×10^6 radians (photons/s/cm^2/surface area), mice were administered × 4 weekly doses of the following treatments by IP injection: PBS, NP (200 µl, 500 µg/ml). Based on the image guided PTT illustrated above, after 24 h, the mice were irradiated with 808 nm or 1064 nm laser in tumor region. LUC signals emanating from the tumors of the animals were imaged periodically. Changes in signal intensities were compared to baseline, were enumerated by gating on the whole peritoneal

cavity, and were determined by measuring the average photon flux in radians, which enabled normalization for differences in imaging areas between mice and in the same mouse over time. The tumor size and body weight were measured every other day. At the last day, major organs (heart, liver, spleen, lung, kidney) and tumors were collected for pathology analysis.

14. Toxicity and systemic side effects

On the 14^{th} day, blood was collected from the healthy BALB/c mice by eyelid blood sampling. The blood samples were centrifuged at 3000 rpm for 15 min to collect plasma, which was further used for analysis of two renal function-related indicators, creatinine (CREA) and urea nitrogen (BUN). For blood biochemical parameter analysis, the obtained plasma samples were measured by an automatic biochemical analyzer. As noted, the blood sample from the untreated mice was used as a control.

15. Statistical analysis.

Data are presented as mean ± SD. Asterisks indicate significant differences (*$p < 0.05$, **$p < 0.01$, ***$p < 0.001$, ****$p < 0.0001$, and ns: not significant), analyzed by unpaired Student's two-sided t test.

Table S1. Composition for polymers used in this study. x+y represents the ratio of conjugated section, while z represents the ratio of non-conjugated section.

Polymer	x+y (conjugated section)	z (non-conjugated section)	Mn	Mw
P0	100%	0%	2774	11228
P10	90%	10%	2799	9637
P30	70%	30%	2726	12430
P70	30%	70%	2458	9480

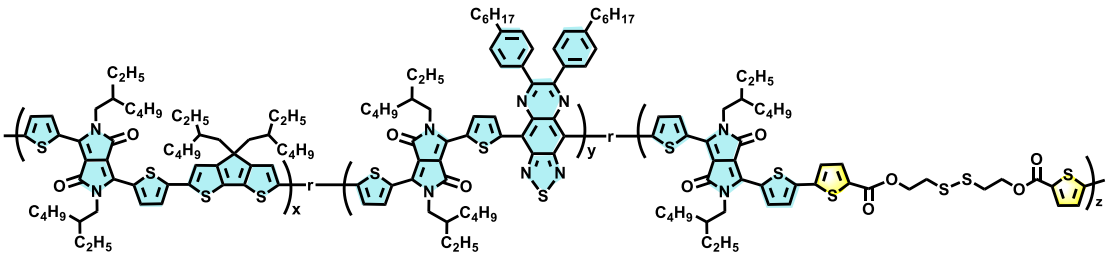

Scheme S1. Chemical structure of polymers used in this study.

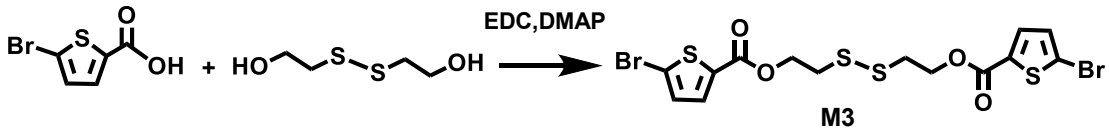

Scheme S2. Synthesis and chemical structure of monomer M3.

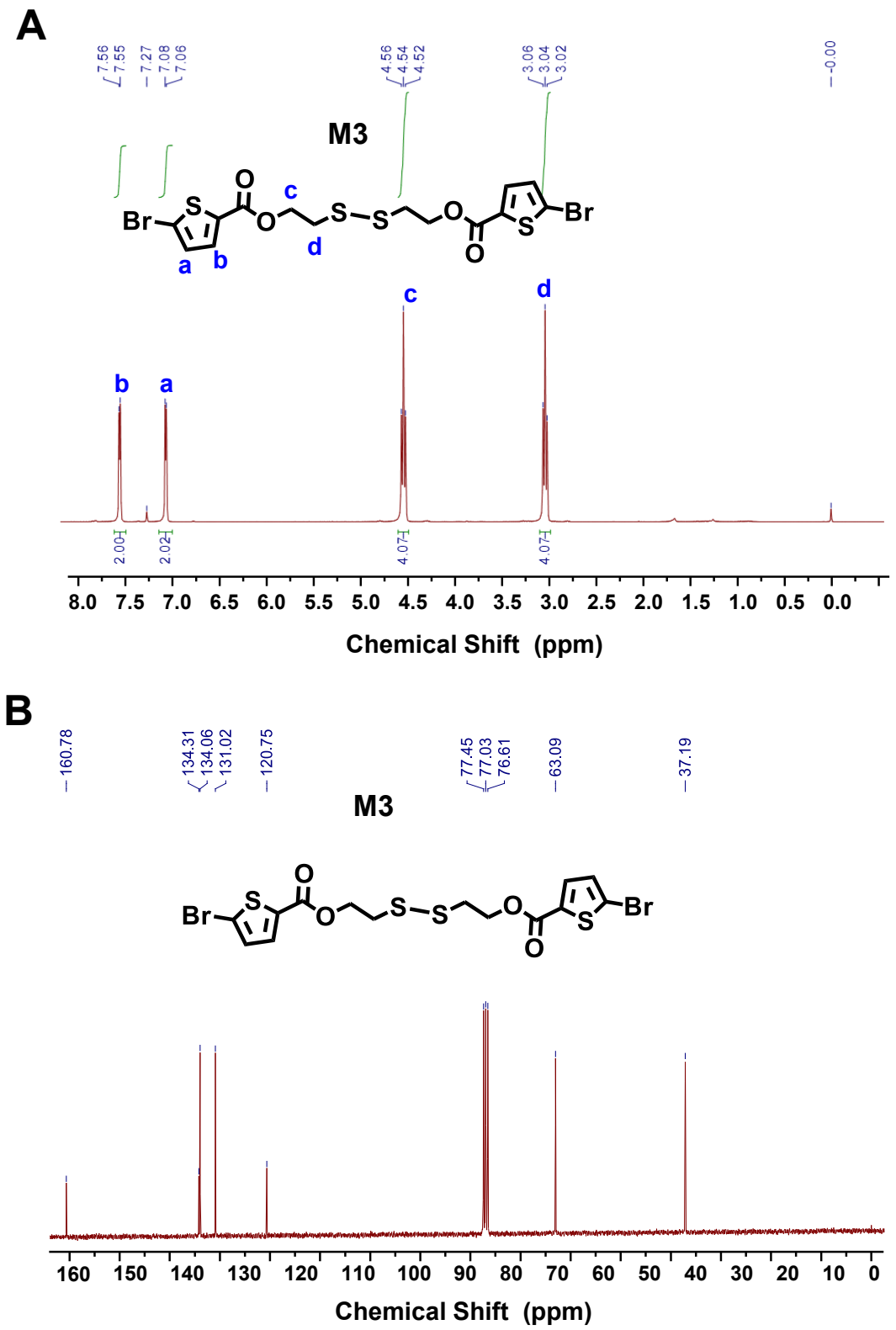

Figure S1. ^{1}H NMR and ^{13}C NMR spectrums of M3 in DMSO-*d6*.

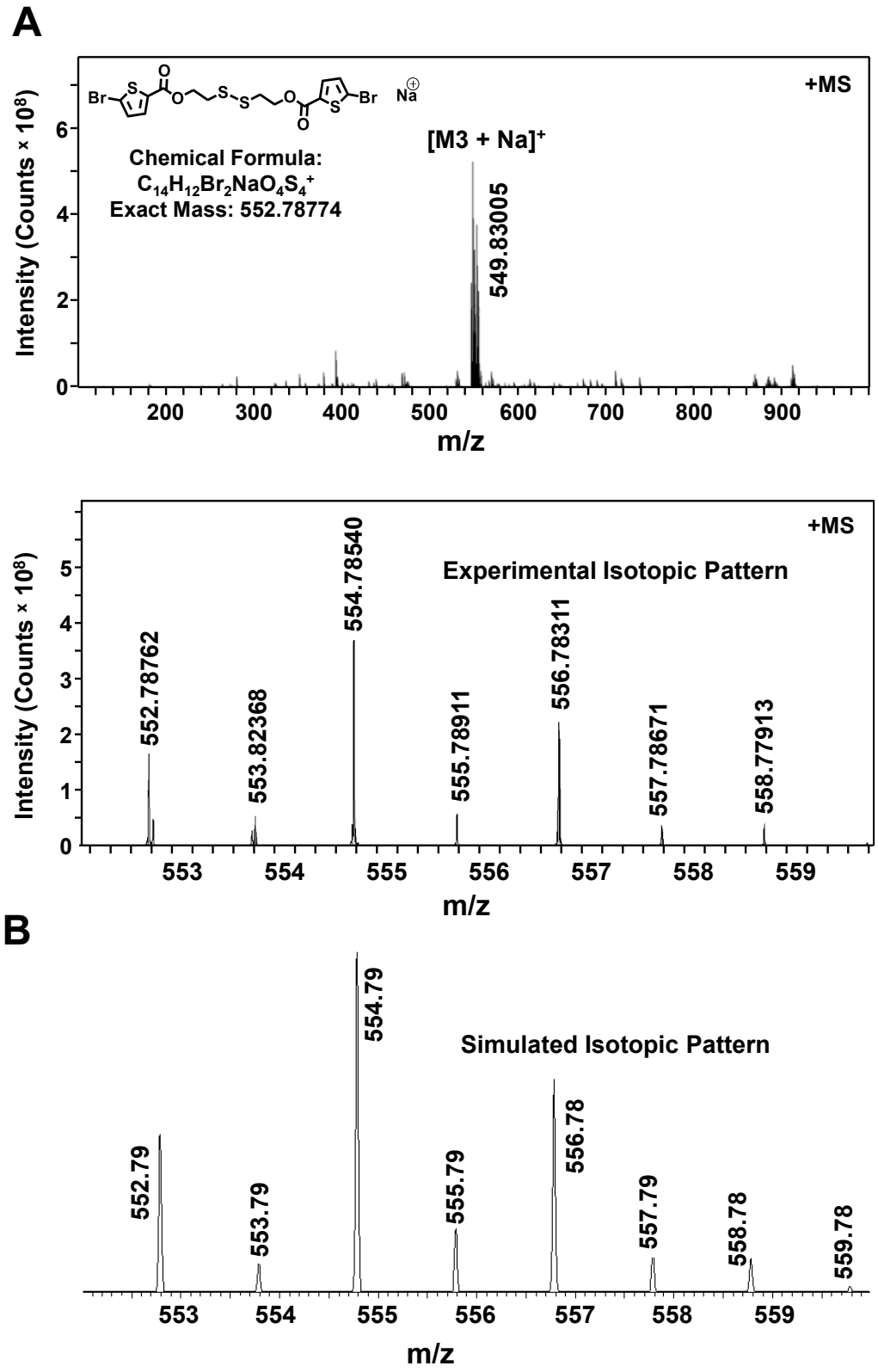

Figure S2. Characterization of M3 by ESI-MS (positive mode). (A) Chemical structure of M3 and the full spectrum as well as the expanded views of experimental isotopic pattern. (B) Simulated isotopic pattern of M3.

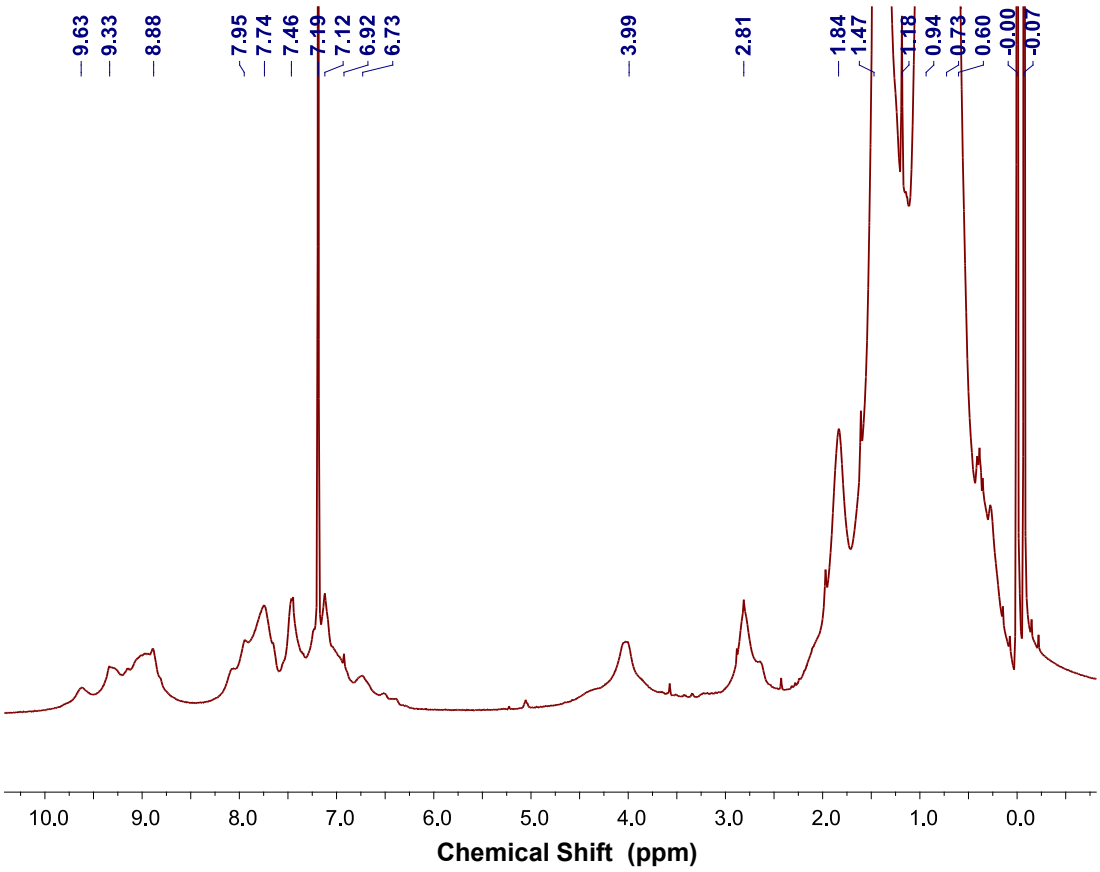

Figure S3. Characterization of P0 by ^{1}H NMR.

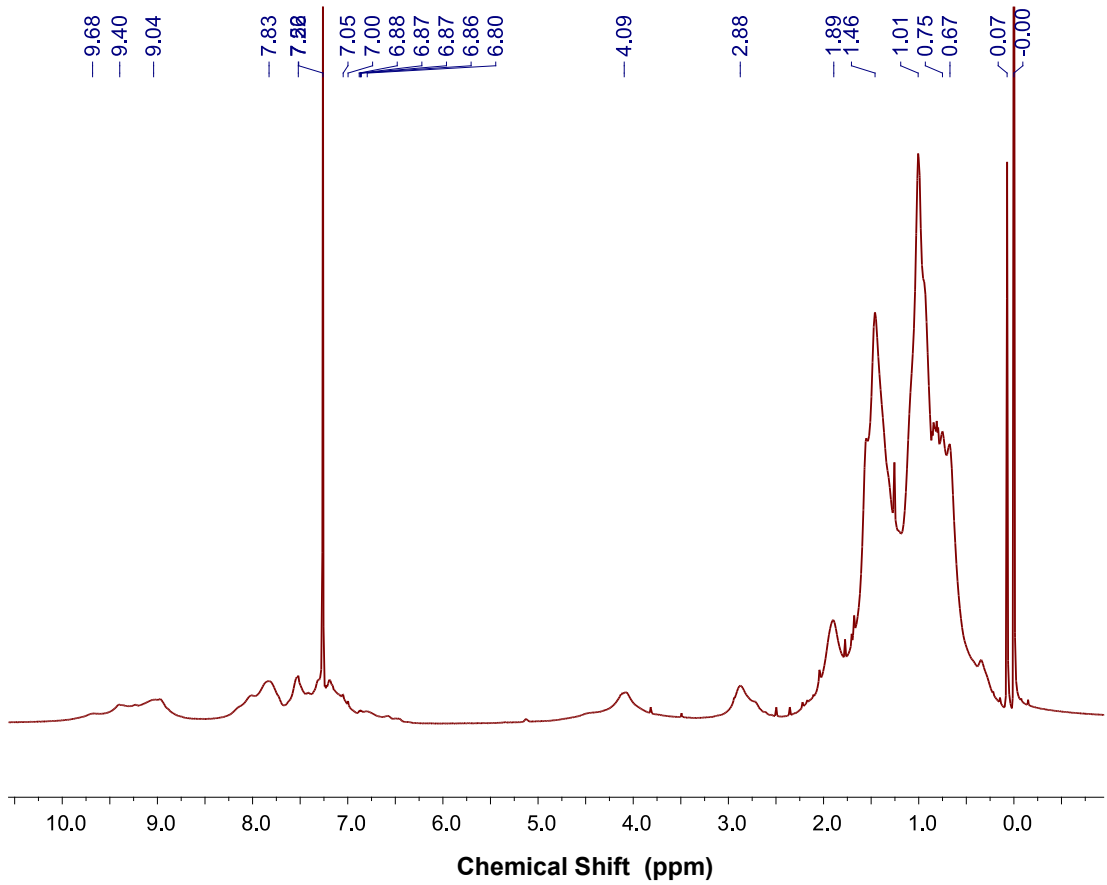

Figure S4. Characterization of P10 by ^{1}H NMR.

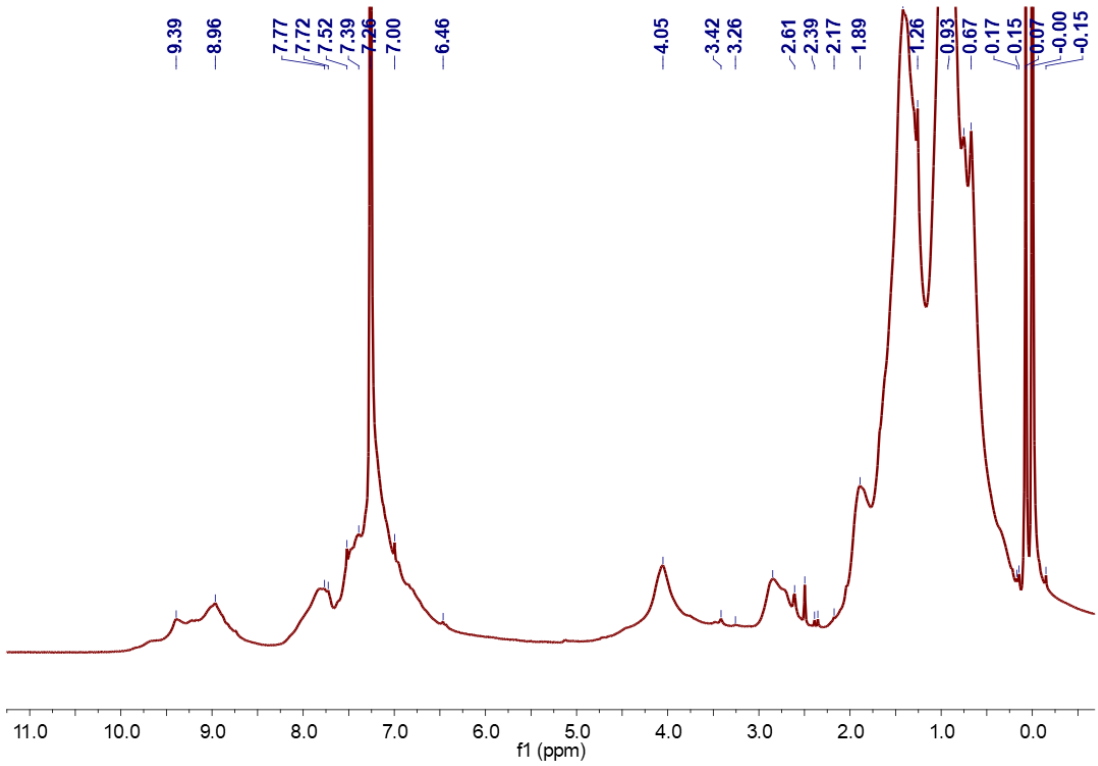

Figure S5. Characterization of P30 by ^{1}H NMR.

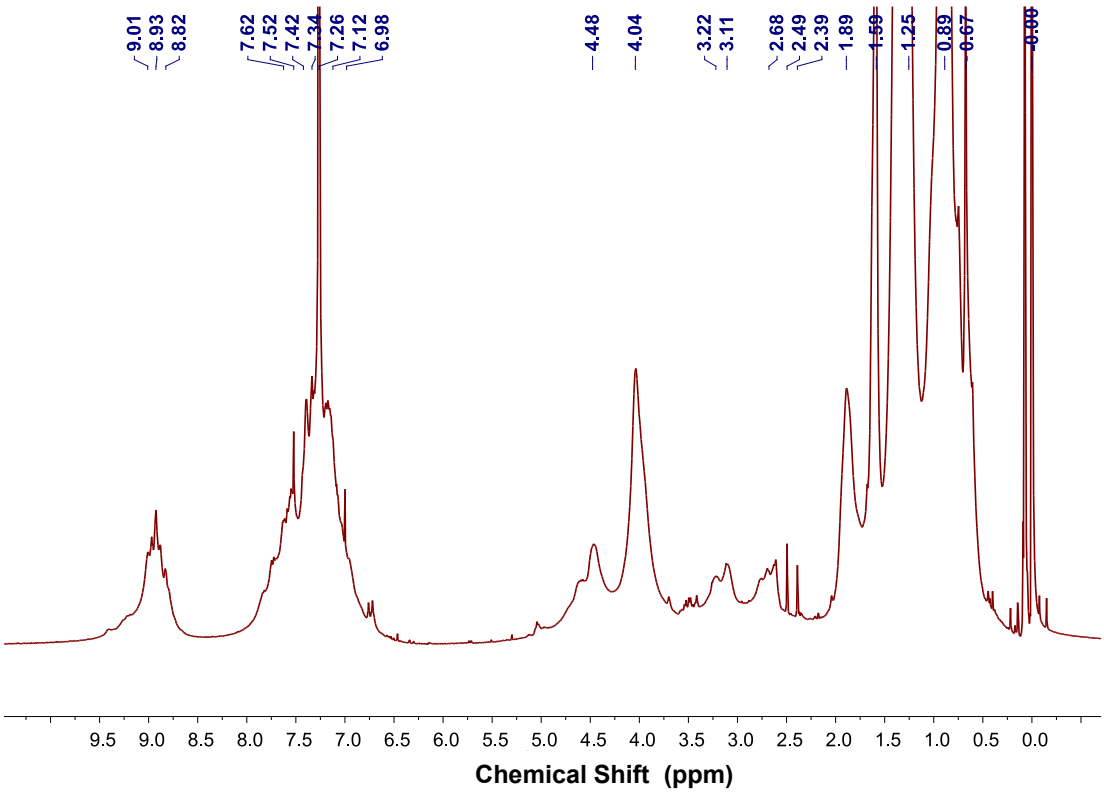

Figure S6. Characterization of P70 by ^{1}H NMR.

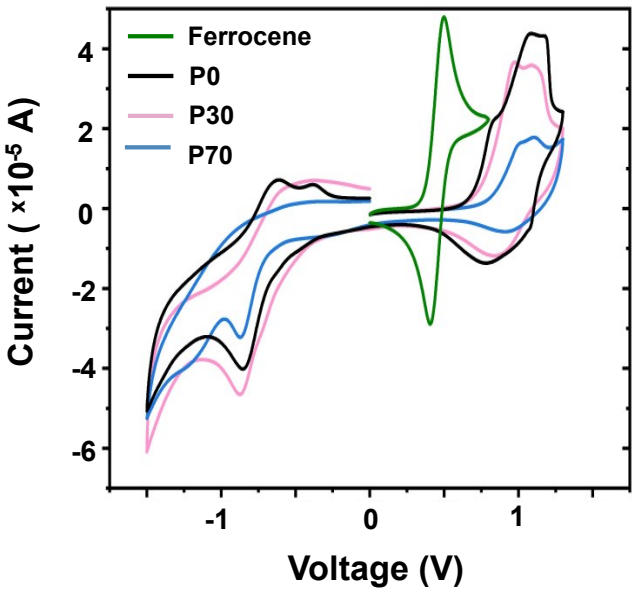

Figure S7. Cyclic voltammetry (CV) measurements for P0, P30, and P70.

Table S2. HOMO and LUMO energies for measured polymer and their bandgaps.

Polymer	E_{LUMO}(eV)[b]	E_{HOMO}(eV)[b]	E_g^{cv}(eV)[c]
P0	-3.87	-5.00	1.13
P30	-3.77	-5.08	1.31
P70	-3.63	-5.15	1.52

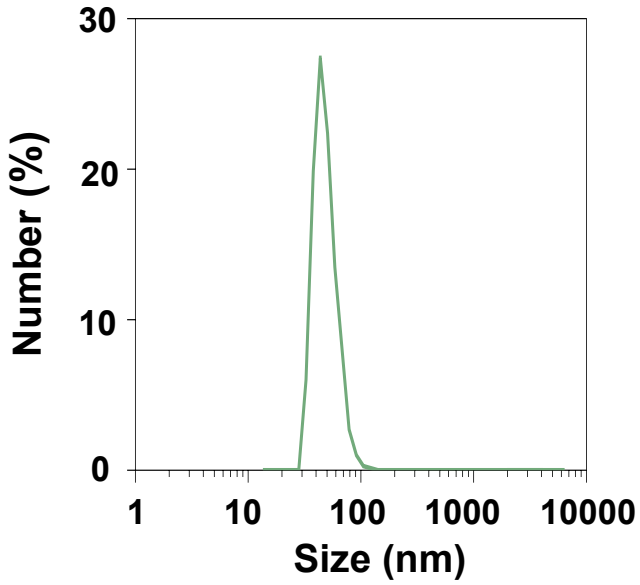

Figure S8. Characterization of NP through DLS.

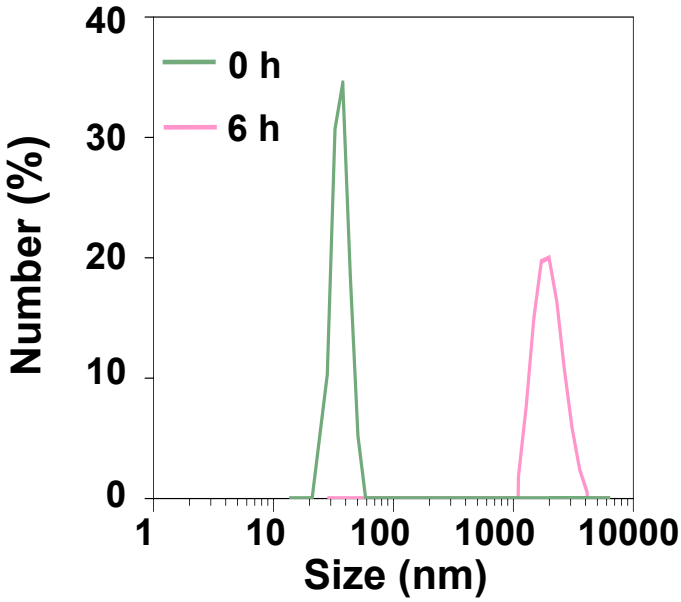

Figure S9. DLS of NP after incubation with GSH.

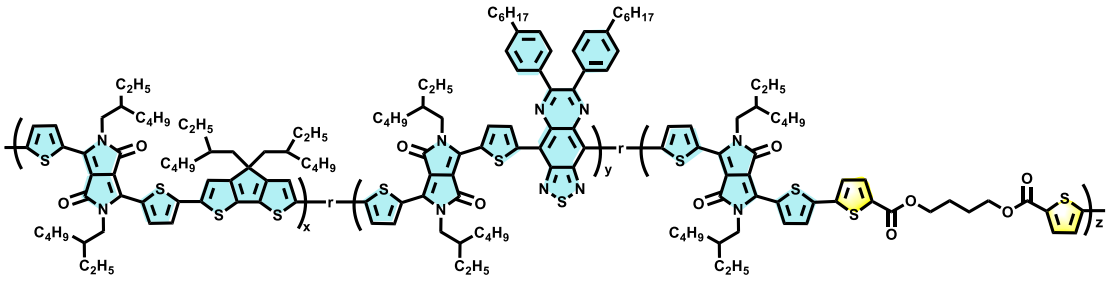

Scheme S3. Chemical structure of non-degradable polymer.

Table S3. Molecular structure of non-degradable polymer.

Polymer	x+y (conjugated section)	z (non-conjugated section)	Mn	Mw
Non-degradable polymer	70%	30%	3910	14301

Scheme S4. Synthesis and chemical structure of non-degradable monomer.

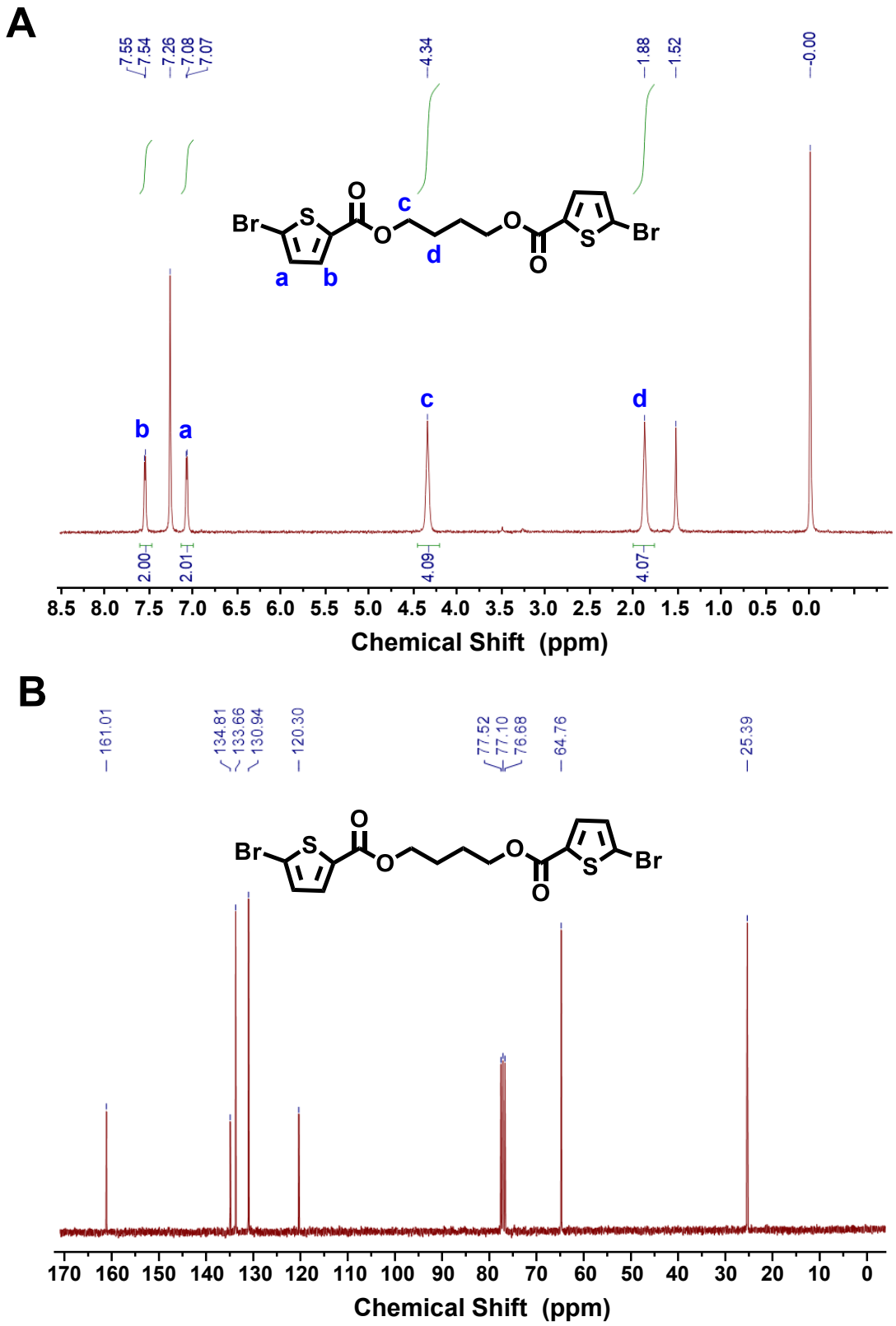

Figure S10. ^{1}H NMR and ^{13}C NMR spectrums of non-degradable monomer in DMSO-*d6*.

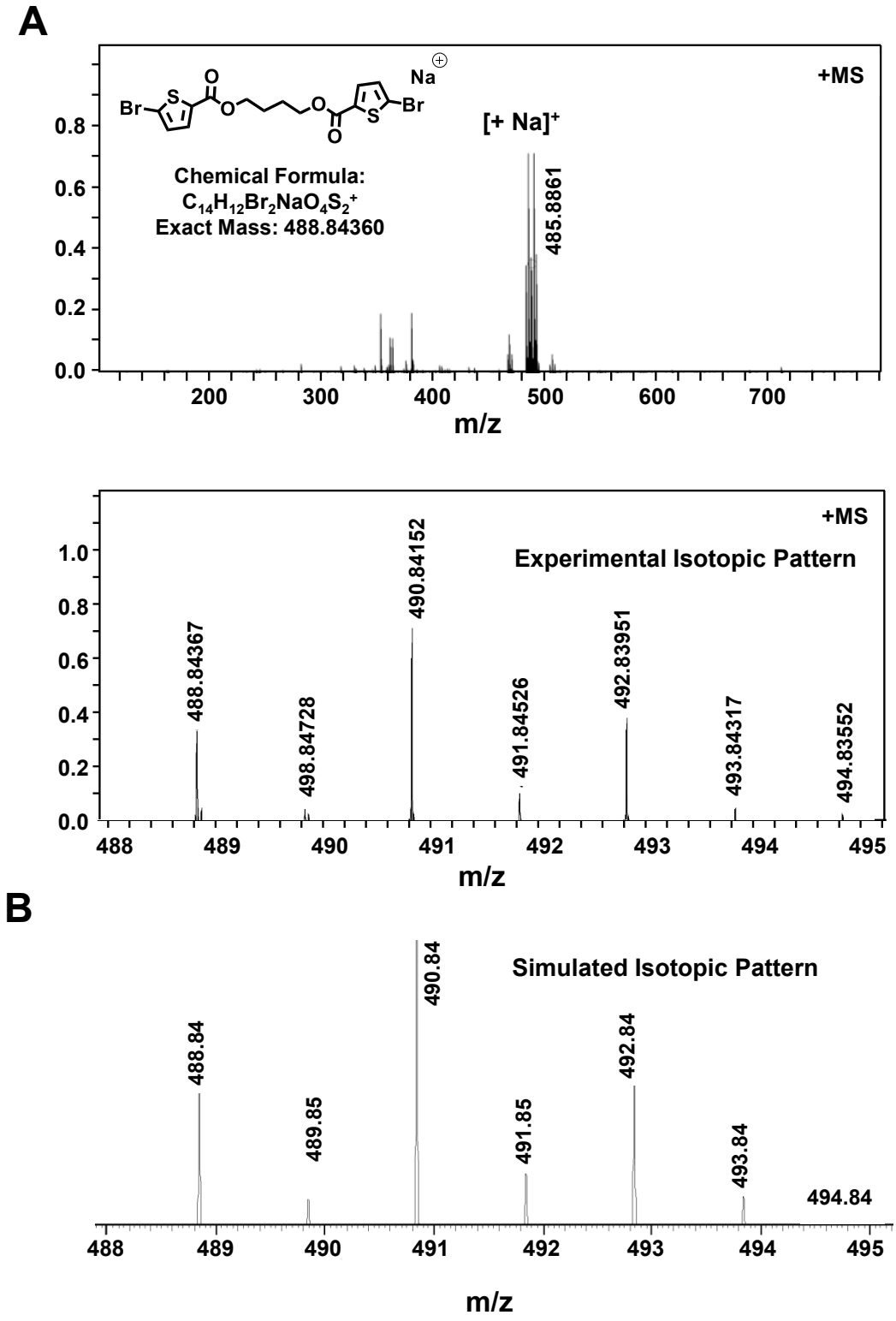

Figure S11. Characterization of non-degradable monomer by ESI-MS (positive mode). (A) Chemical structure of monomer and the full spectrum as well as the expanded views of experimental isotopic pattern. (B) Simulated isotopic pattern of non-degradable monomer.

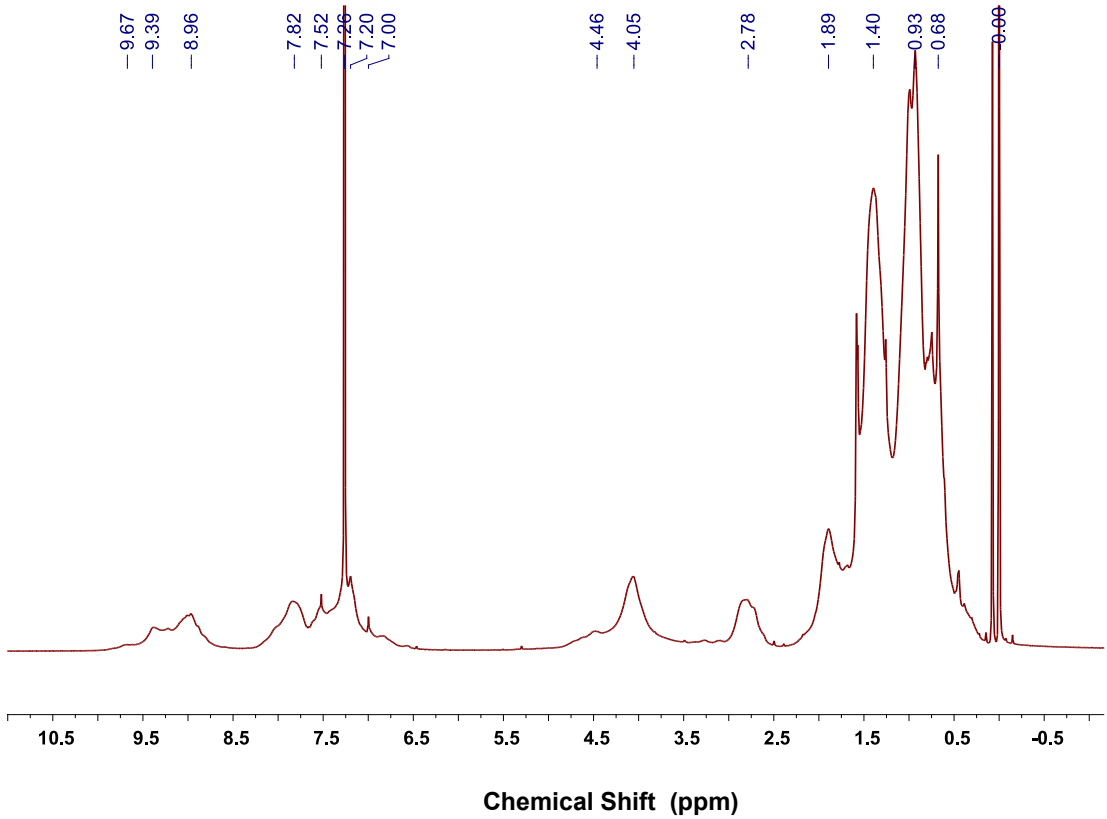

Figure S12. Characterization of non-degradable polymer by ^{1}H NMR.

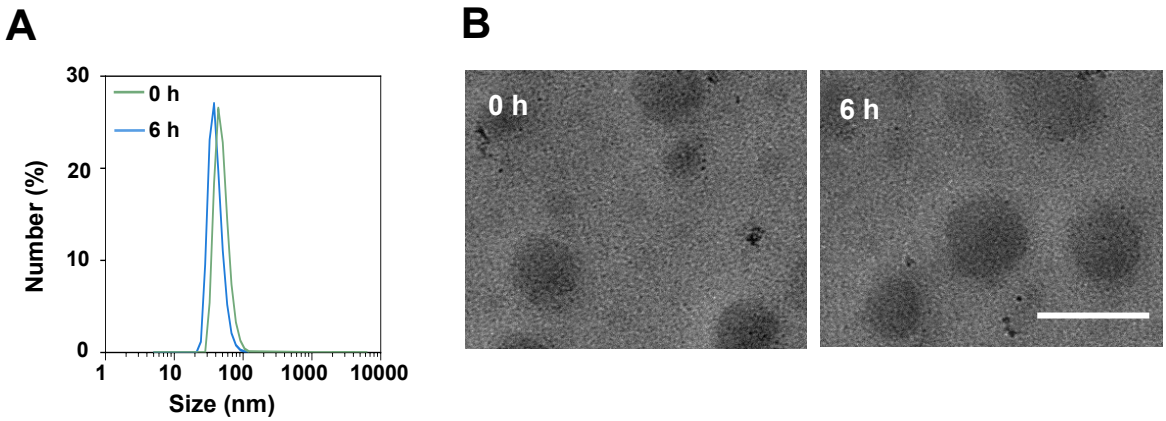

Figure S13. (B) DLS and (C) TEM result for the degradation process of non-degradable NP with or without GSH incubation. Scale bar: 100 nm.

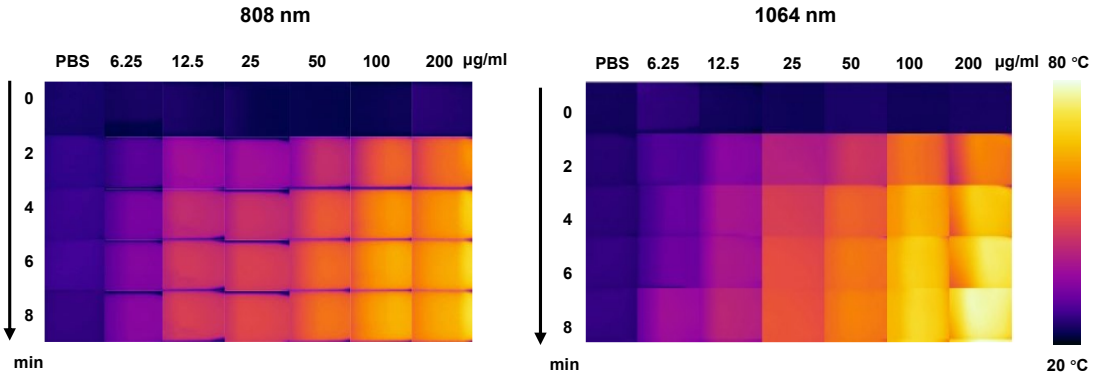

Figure S14. IR Thermal image for non-degradable NP under 8 min illumination of 808 nm and 1064 nm laser (1W cm^{-2}).

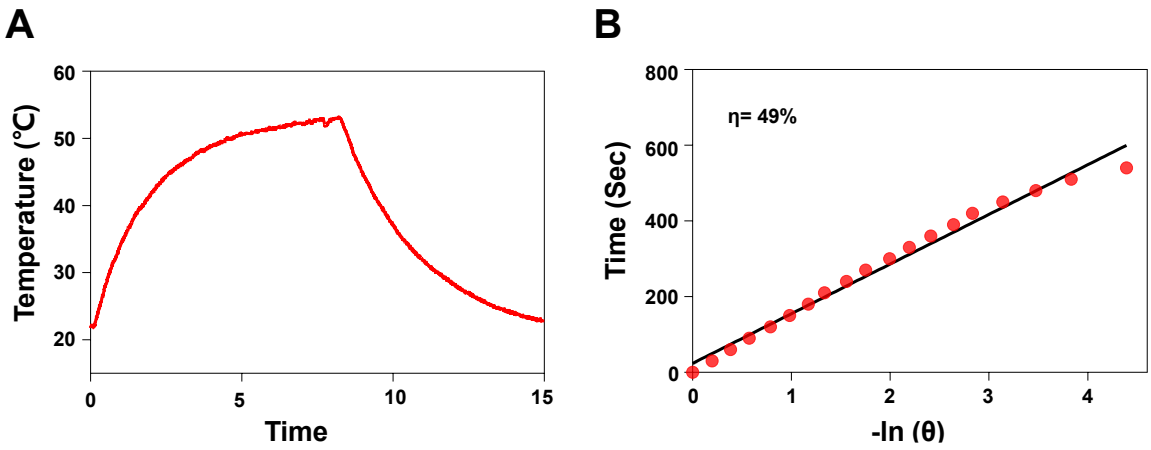

Figure S15. (A) Photothermal response of NP at the concentration of 25 µg mL^{-1} under 1064 nm laser irradiation (1 W cm^{-2}), followed by switching off the laser. (B) Linear time data versus -ln(θ) obtained from the cooling curve.

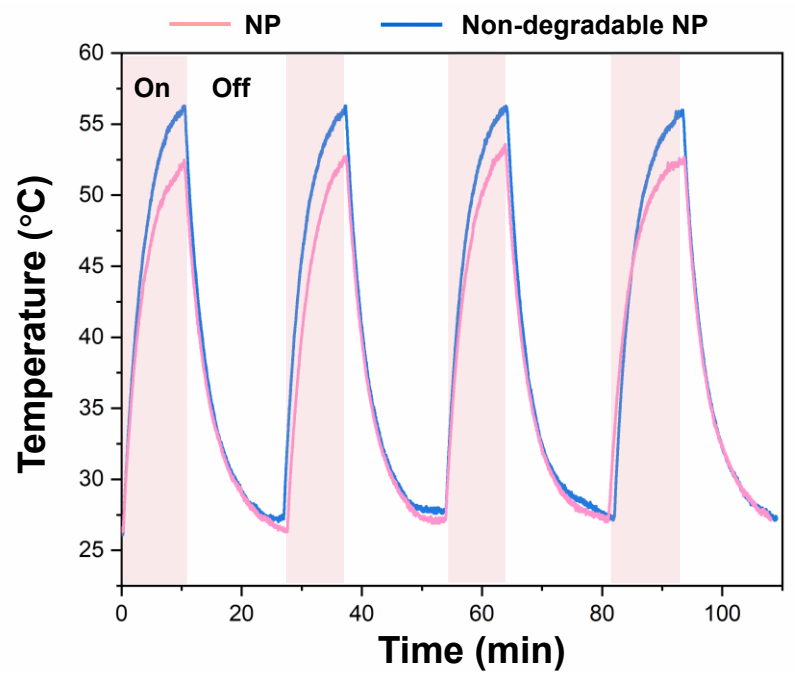

Figure S16. Photothermic stability of NP and non-degradable NP upon 1064 nm laser irradiation of 1 W cm^{-2} for four on/off cycles.

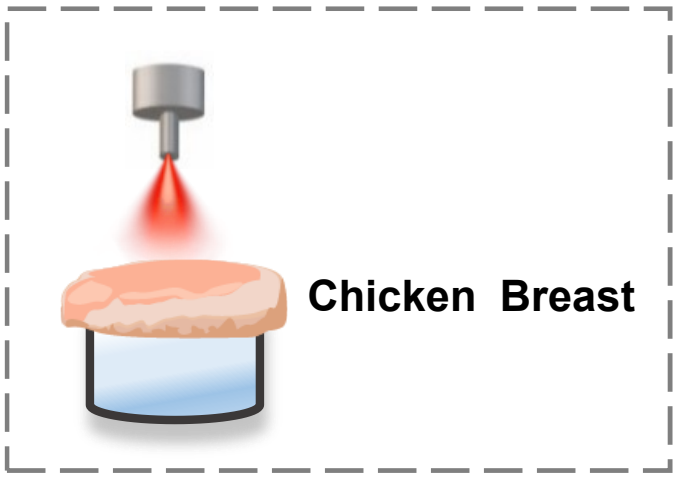

Scheme S5. Schematic showing the coverage of solutions with a chicken breast with different thickness.

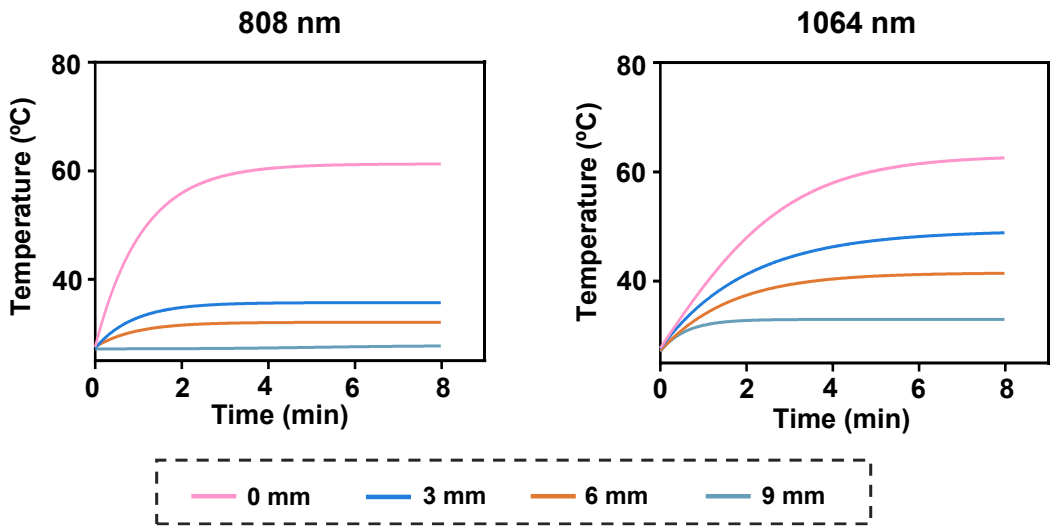

Figure S17. Heating curve of NP solution (100 μg ml^{-1}) at different depth thickness (0, 3, 6, and 9 mm) of chicken breast under 808 and 1064 nm laser.

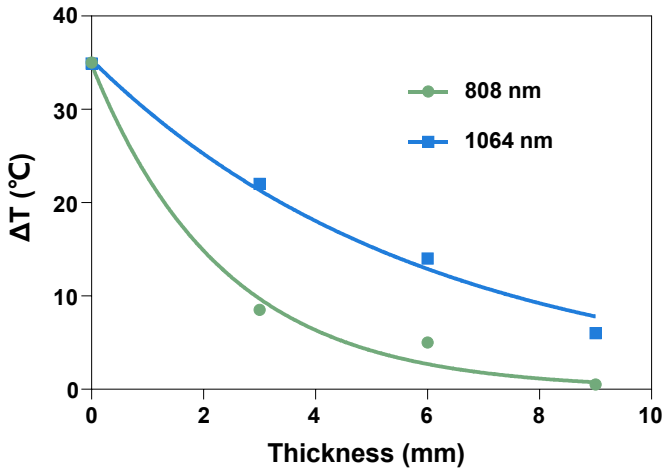

Figure S18. Fitted exponential decay of temperature change of NP solution (100 μg/mL) at different depths of chicken breast tissue.

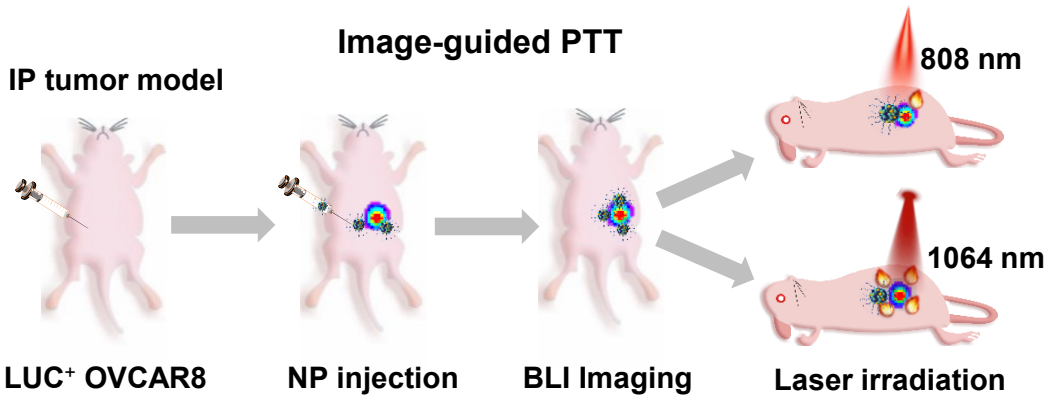

Scheme S6. Schematic showing the process of image-guided PTT.

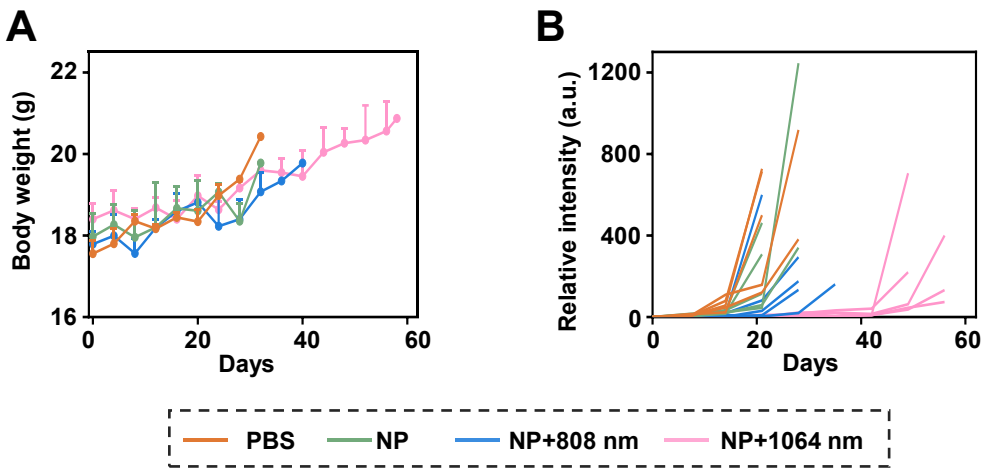

Figure S19. (A) Body weight and (B) tumor burden over time as determined by changes from the baseline radiant flux associated with the BLI signal intensity inhibition.

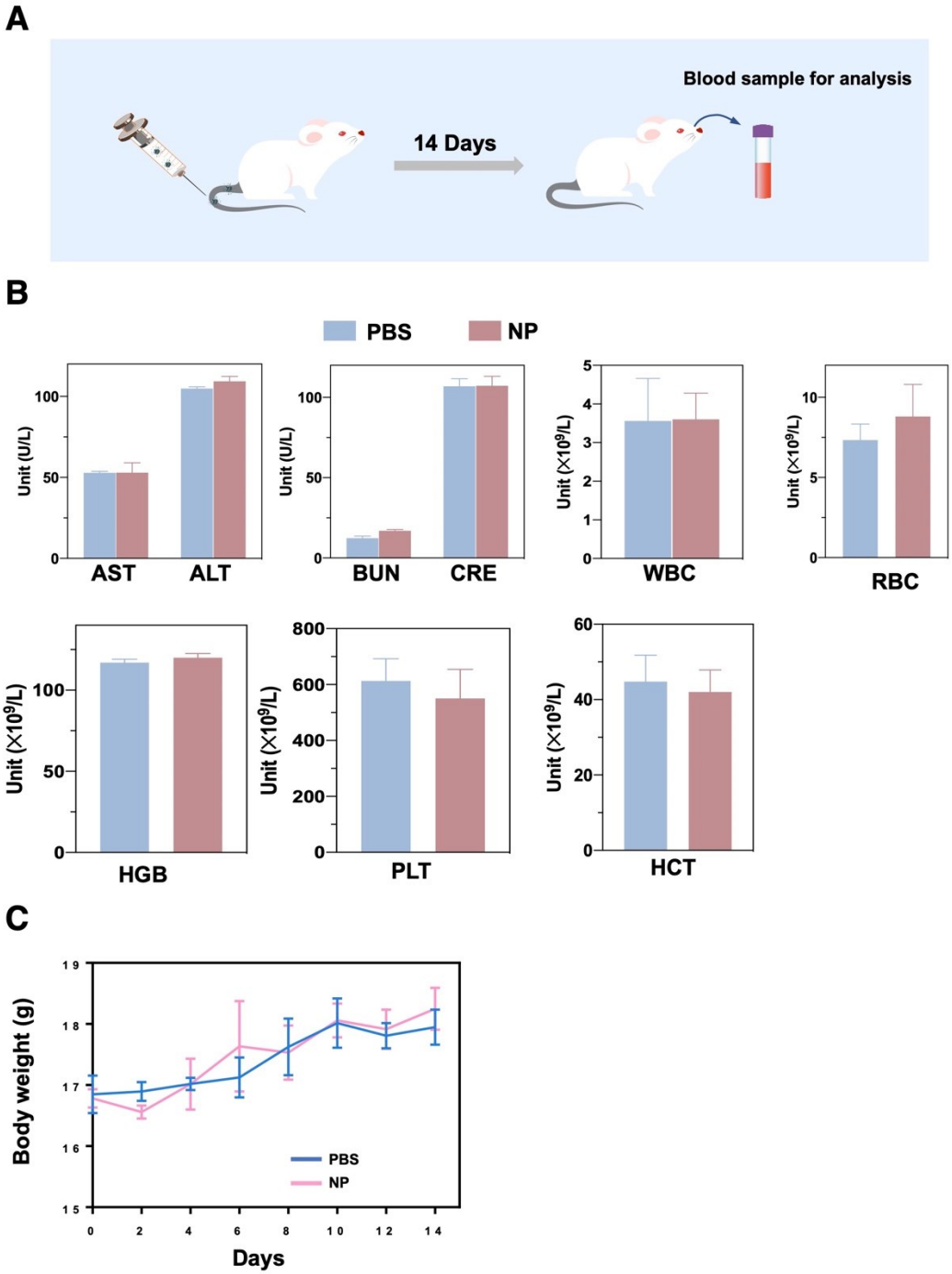

Figure S20. *In vivo* systemic toxicities study. The BALB/c mice were randomly grouped (n=3 mice per group), and treated with a single dose of PBS, NP at 10 mg kg^{-1} *via i.v.* injection. (A) Schematic illustration for the process of biosafety study. (B) the serology panel for biomarkers of body function. (C) Body weight changes of mice.

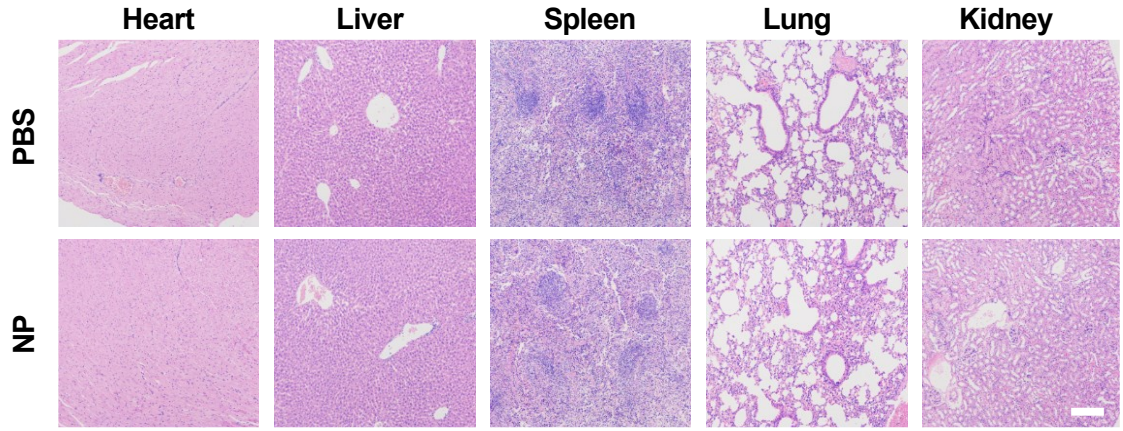

Figure S21. H&E study of major organs for systematic toxicity study. Scale bar: 200 μm.